

Predator-prey dynamics: Chasing by stochastic resetting

J. Quetzalcóatl Toledo-Marín,^{1,*} Denis Boyer,^{1,†} and Francisco J. Sevilla^{1,‡}

¹*Instituto de Física, Universidad Nacional Autónoma de México,
Apartado Postal 20-364, 01000 México, Ciudad de México, México*

(Dated: June 11, 2021)

We analyze predator-prey dynamics in one dimension in which a Brownian predator adopts a chasing strategy that consists in stochastically resetting its current position to locations previously visited by a diffusive prey. We study three different chasing strategies, namely, *active*, *uniform* and *passive* which lead to different diffusive behaviors of the predator in the absence of capture. When capture is considered, regardless of the chasing strategy, the mean first-encounter time is finite and decreases with the resetting rate. This model illustrates how the use of cues significantly improves the efficiency of random searches. We compare numerical simulations with analytical calculations and find excellent agreement.

Stochastic processes subject to resetting exhibit diffusive and first passage properties that markedly differ from ordinary diffusion [1–7]. When a Brownian particle is occasionally reset to a fixed position in space, the mean first passage time to a given target becomes finite and can be minimized with respect to the resetting rate [1]. Random searches based on resetting principles are advantageous in many contexts [4, 6], including situations where many targets or resetting points are distributed in space [2].

The statistics of first encounter times is key to understand reaction kinetics between freely diffusive molecules or prey/predators dynamics [8–12]. In the latter context, prey capture can involve relatively complex decisions by the predator depending on the position of the prey, or vice-versa [13, 14]. For instance, this is the case when the predator uses information about positions occupied by a prey, and decides to relocate to regions of space where it is more likely to be found [15]. There are other phenomena, such as olfaction in the case of olfaction-driven navigation in animals [15–17], backtrack recovery in RNA polymerases [18, 19] or the formation of physical contacts between distant segments of DNA by means of temporal and spatial motion scales [20], that can be modeled by a searcher influenced by cues whose spatial distribution is time dependent.

In this Letter we address a problem of two interacting Brownian particles for which the dynamics of one of them, called the *predator*, is subordinated to the dynamics of the other, called the *prey*, in one-dimensional space. In the following we will phrase the problem in terms of prey and predator for clarity. The chasing dynamics of the predator consist of frequent relocations to positions previously visited by the prey. In other words, this resetting dynamics correspond to a non-Markovian search process in which the predator stochastically visits previous prey positions. Prey motion is not influenced by the predator here. We focus on the effects of the predator search strategy on its own diffusion and on the statistics of first encounter times with the prey [21]. Our results may also be relevant in collective animal movement phenomena [22–25].

For this problem, we show that for a finite reset rate, the mean capture time is finite, contrary to the situation when the predator simply diffuses without resetting for which, as is well known, the mean capture-time diverges [12, 24].

We model the prey’s dynamics as an overdamped Brownian motion of a free particle diffusing in one dimensional space. The time evolution of the prey’s position, $y(t)$, is given by the stochastic differential equation

$$\frac{d}{dt}y(t) = \xi_y(t), \quad (1)$$

where $\xi_y(t)$ denotes a Gaussian-white noise, with mean $\langle \xi_y(t) \rangle = 0$, and autocorrelation function $\langle \xi_y(t)\xi_y(s) \rangle = 2D_y\delta(t-s)$, D_y being the prey’s diffusion coefficient and $\delta(t)$ the Dirac’s delta function.

The predator’s dynamics is modeled by the overdamped motion of a Brownian particle that randomly jumps from time to time, to a position previously visited by the prey, which makes the subordination process explicit. The time evolution of the predator’s position, $x(t)$, is determined by the following stochastic differential equation

$$\frac{d}{dt}x(t) = \xi_x(t)[1 - \sigma(t)] + \zeta[t, y(s); s \leq t]\sigma(t), \quad (2)$$

that describes the intermittent process of the predator dynamics. We consider the simplest case for the stochastic process $\xi_x(t)$, taken as an unbiased Gaussian-white noise, i.e. $\langle \xi_x(t) \rangle = 0$ and $\langle \xi_x(t)\xi_x(s) \rangle = 2D_x\delta(t-s)$, where D_x denotes the intrinsic diffusion coefficient of the predator. $\sigma(t)$ is a dichotomic stochastic process that takes the values 1 at a Poisson rate Q . $\zeta[t, y(s); s \leq t]$ denotes the stochastic discontinuous process that describes the predator chasing dynamics, namely, at a constant rate Q , the predator jumps from its current position $x(t)$, to a position $y(s)$ previously visited by the prey at the random time $s \leq t$ (as depicted in Fig. 1), the random variable s being distributed according to the probability density $\phi(s; t)$. This kernel entails the information that the predator has about past positions of the prey, which

we will refer henceforth, as the predator's memory. If the predator has unbiased complete memory, any previous time s is equally probable in the time interval $[0, t]$. Similar memory kernels have been considered in other models, such as the *elephant* random walk [26, 27] or the preferential visit model [28].

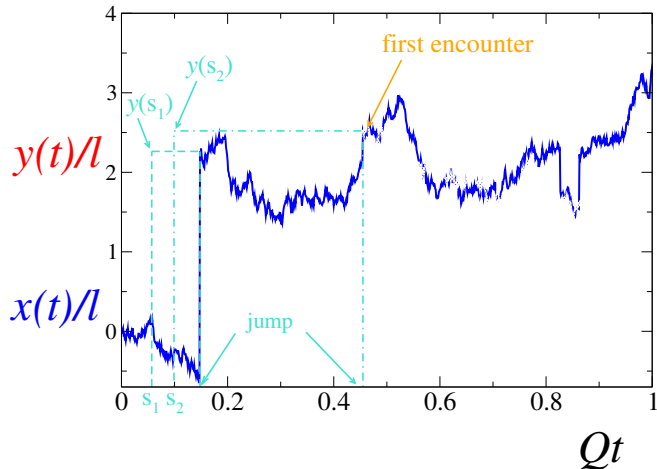


FIG. 1. Prey and predator dimensionless trajectories, $y(t)/l$ (red), $x(t)/l$ (blue) respectively, for the case when predators and prey diffusion constants are the same $D_x = D_y$. l denotes the length scale $\sqrt{D_y/Q}$. The first two jumps of the predator are marked with arrows at $Qt \approx 0.148$ and $Qt \approx 0.455$. In the first jump the predator chooses (from a uniform distribution) to jump to the previously position visited by the prey $y(s_1)$ where s_1 (≈ 0.057) is chosen from a uniform distribution in the interval $[0, 0.148]$. In this example the predator encounters for the first time the prey just right after the second jump (pointed with the orange arrow).

We first focus on the predator dynamics induced by the chasing when no capture of the prey is considered. In such a case, the stochastic processes defined by Eqs. (1) and (2) are equivalently formulated in terms of the conditional probability density functions $P(y, t|y_0)$, $\Pi(x, t|x_0)$. The prey's diffusion propagator at time t , $P(y, t|y_0)$, is given by $G_{D_y}(y, t|y_0) = \exp\{-(y - y_0)^2/4D_y t\}/\sqrt{4\pi D_y t}$, which is the Gaussian distribution, solution of the diffusion equation with diffusion coefficient D_y and the initial condition $G_{D_y}(y, t = 0|y_0) = \delta(y - y_0)$. The predator diffusion propagator, $\Pi(x, t|x_0)$, on the other hand, is given by the solution of the Fokker-Planck equation

$$\frac{\partial}{\partial t}\Pi(x, t|x_0) = D_x \frac{\partial^2}{\partial x^2}\Pi(x, t|x_0) - Q\Pi(x, t|x_0) + Q \int_0^t ds \phi(s; t) P(x, s|y_0), \quad (3)$$

with the initial distribution $\Pi(x, t = 0|x_0) = \delta(x - x_0)$. $\phi(s; t)$ gives the probability density of choosing the time instant s in the interval $[0, t]$. The first term in the right-

hand side of Eq. (3) corresponds to the predator diffusion process, while the second and third terms refer to the resetting process in which the predator jumps to a position previously visited by the prey, where $P(y, t)dy$ gives the probability of the prey being at $\{y, y + dy\}$ at time t . Equation (3) is akin to the continuous-space and continuous-time diffusion process under resetting with memory studied in Ref. [29]. In the present study, the subordination to the prey's dynamics leads to new qualitative features as is discussed afterwards.

The statistical properties of the predator diffusion process are derived from $\Pi(x, t|x_0)$. The solution of Eq. (3) for arbitrary resetting strategy $\phi(s; t)$ is given by

$$\Pi(x, t|x_0) = e^{-Qt}G_{D_x}(x, t|x_0) + Q \int_0^t ds e^{-Q(t-s)} \times \int_0^s ds' \phi(s'; s) G_{D_y}\left(x, \frac{D_x}{D_y}(t-s) + s' \middle| y_0\right), \quad (4)$$

As is expected, the Gaussian distribution $G_{D_x}(x, t|x_0)$ for the distribution of the predator positions is recovered from (4) by setting $Q = 0$. At finite Q and in the long-time regime, $Qt \gg 1$, Eq. (4) reads

$$\Pi(x, t) \sim \int_{-\infty}^{\infty} dx' L_{l_x}(x - x') \int_0^t ds \phi(s; t) G_{D_y}(x', s|y_0), \quad (5)$$

(see SM in Ref. [30]). $L_{l_x}(x)$ denotes the Laplace distribution that occurs in the related diffusion process of a Brownian particle that stochastically resets its position to the origin [1], given by $\exp\{-|x|/l_x\}/2l_x$, with $l_x = \sqrt{D_x/Q}$ the characteristic distance the predator travels between consecutive resetting. If this is vanishingly small, i.e., when either the resetting rate is large enough or the predator diffusion coefficient is small enough, $L_{l_x}(x - x')$ becomes sharply distributed around x , thus leading to $\Pi(x, t) \sim \int_0^t ds \phi(s; t) G_{D_y}(x, s|y_0)$.

From Eq. (4) the first two moments can be obtained for arbitrary strategy $\phi(s; t)$, these are given explicitly by

$$\langle x(t) \rangle = x_0 e^{-Qt} + y_0 (1 - e^{-Qt}), \quad (6a)$$

$$\langle x^2(t) \rangle = x_0^2 e^{-Qt} + \left(y_0^2 + \frac{2D_x}{Q}\right) (1 - e^{-Qt}) + 2D_y Q \int_0^t ds e^{-Q(t-s)} \bar{\tau}(s), \quad (6b)$$

where $\bar{\tau}(t)$ denotes the mean time of the distribution $\phi(\tau; t)$ given by the expression

$$\bar{\tau}(t) = \int_0^t d\tau \tau \phi(\tau; t). \quad (7)$$

From expression (6a) it can be deduced that: The average position of the predator is independent on the resetting strategy $\phi(s; t)$ and tends exponentially fast toward the

initial position of the prey, y_0 ; in the short-time regime it is given by $x_0 + (y_0 - x_0)Qt$, i.e., the predator travels on average ballistically with velocity $(y_0 - x_0)Q$.

We now specify these results for an illustrative case, namely, with exponential resetting strategies, where the probability density of picking an instant s in $[0, t]$ is given by

$$\phi(s; t) = \frac{\lambda e^{-\lambda s}}{1 - e^{-\lambda t}}, \quad (8)$$

with λ a real parameter in $(-\infty, \infty)$ that marks the range of the memory. For $\lambda < 0$, the chasing strategy is denoted as *active*, i.e., it is based on a short-term memory as the predator relocates with a large probability to the most recent positions visited by the prey. The $\lambda = 0$ case corresponds to a uniform memory, for which any instant s in the period of time $[0, t]$ is chosen with the same probability weight [26, 28]. The scenario given by $\lambda > 0$ corresponds to a *passive* chasing strategy, for which the predator relocates preferentially to the initial positions visited by the prey.

The predator's mean-squared displacement (6b), depends on the resetting strategy chosen through $\bar{\tau}(t)$. For the long-term memory strategy ($\lambda > 0$) and $Qt \gg 1$, we have $\bar{\tau}(t) \rightarrow \lambda^{-1}$, and thus the mean-squared displacement saturates $\langle x^2(t) \rangle - \left(y_0^2 + \frac{2D_x}{Q}\right) \approx 2D_y\lambda^{-1}$ (see Fig. 2), i.e., the predator gets trapped around the prey initial position, similarly to the process with stochastic resetting to the origin [1]. In the limit $\lambda \rightarrow \infty$, $\phi(s; t) \rightarrow \delta(s)$, thus, the predator stochastically resets to the prey's initial position, y_0 , and asymptotically we have $\Pi(x) = L_{l_x}(x - y_0)$, which corresponds to the stationary probability distribution found in Ref. [1].

For $\lambda = 0$, we have normal diffusion in the large-time limit, since $\langle x^2(t) \rangle \sim D_y t$, however, the kurtosis of $\Pi(x, t)$ approaches asymptotically to 4 indicating that it is not Gaussian. Therefore, this case belongs to a class of diffusion processes known as *Brownian yet non-Gaussian diffusion* [31], for which the probability distribution is not Gaussian in the long-time regime [see Eq. (5)]. Remarkably, the predator's diffuses with an effective diffusion coefficient that is half of the prey.

For the short-term strategy, $\lambda < 0$, the predator jumps to positions recently visited by the prey, which at large times yields linear-time dependence $\langle x^2(t) \rangle \sim 2D_y t$, which indicates that the predator diffuses with the same diffusivity as the prey. In the supplemental material (see Ref. [30]) we provide the explicit form of the mean squared displacement. In Fig. 2 we compare the time-dependence of the mean-squared displacement obtained from numerical simulations with Eq. (6b) for which we see an excellent agreement.

We continue our analysis in the scenario for which the predator captures the prey upon first encounter, and we study the statistics of these first encounter times. In

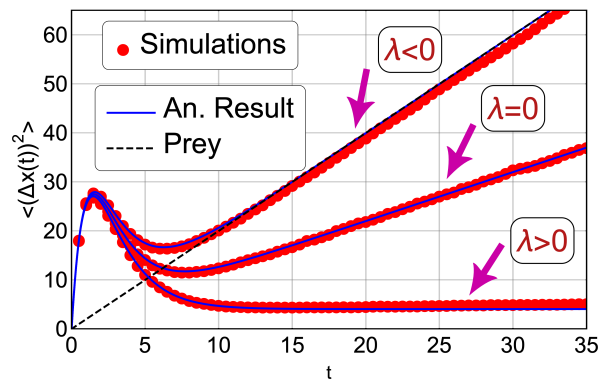


FIG. 2. Mean squared displacement of the predator as a function of time with $x_0 = 0$, $y_0 = 10$, $D_x = 1$, $D_y = 1$, $Q = 0.5$ and $\langle (\Delta x)^2 \rangle = \langle x^2(t) \rangle - \left(y_0^2 + \frac{2D_x}{Q}\right)$. The red dots were obtained by simulations, while the blue curves correspond to Eq. (6b). Notice that for large time, i.e., $t \gg 1/Q$, the mean square displacement (MSD) of the predator goes as $1/\lambda$, $D_y t$ and $2D_y t$ when $\lambda > 0$, $\lambda = 0$ and $\lambda < 0$, respectively, as shown in Eq. (6b). The MSD for the prey (dashed lines) is shown for reference.

the absence of the resetting process, the first-encounter time distribution reduces to the Lévy-Smirnov distribution $f(t; \mathcal{T}_0) = (\mathcal{T}_0/4\pi t^3)^{1/2} \exp\{-\mathcal{T}_0/4t\}$, where $\mathcal{T}_0 = z_0^2/(D_x + D_y)$ and z_0 is the initial relative distance between the prey and the predator. In the long-time regime, such distribution is characterized by the long tail $f_0(t; \mathcal{T}_0) \sim t^{-3/2}$, which implies the nonexistence of the mean encounter time [12]. The predator resetting process induces a *renewal* of the first-encounter time process, i.e., after the n -th resetting event the Lévy-Smirnov distribution turns into $f(t; \mathcal{T}_n)$, where \mathcal{T}_n is obtained by substituting z_0 by $z_n = |x_n - y_n|$, the relative distance between the predator and the prey just right after the stochastic relocation of the predator position. Additionally, this *renewal* process frustrates the long tail of the Levy distribution giving way to a finite mean-encounter time. We show numerical evidence of this in Fig. 3 for all values of λ and finite Q , where we have plotted the dimensionless mean encounter time, $\langle t \rangle$. We further support this finding with arguments based on approximated analytical calculations.

The mean first-passage time can be computed from the survival probability $\mathcal{S}_Q(z_0, t)$, which can be written as a sum, over the number of resets, of the survival probability of a process with exactly n resets. We denote the latter as $\mathcal{S}^{(n)}(z_0, t)$ (see the SM in Ref. [30] for details on the derivation). For a given sequence of the predator position relocations, $\mathcal{S}^{(n)}(z_0, t)$ may be expressed as the convolution of the survival probabilities of the diffusive process between two successive reset events, $\mathcal{S}(z_i, t_i)$, multiplied by the probability that a reset event does not occur. Notice that the survival probability between any two consec-

utive resets is simply the survival probability at time t_i of a Brownian particle with initial position z_i and diffusivity $D = D_x + D_y$, *viz.* $\mathcal{S}(z_i, t_i) = \mathbf{Erf}(|z_i|/\sqrt{4Dt_i})$, where $\mathbf{Erf}(\bullet)$ is the error function. In Laplace domain we have

$$\tilde{\mathcal{S}}_Q(z_0, \{z_i\}, u) = \tilde{\mathcal{S}}(z_0, Q + u) \times \left(1 + \sum_{n=1}^{\infty} \prod_{i=1}^n [Q \tilde{\mathcal{S}}(z_i, Q + u)] \right). \quad (9)$$

In the above expression, we have fixed z_i , which are the relative distance once the i^{th} reset event occurs. The function $\tilde{\mathcal{S}}(z_0, u)$ is the Laplace transform of the survival probability of the process without reset, namely,

$$\tilde{\mathcal{S}}(z_0, u) = \frac{1}{u} \left(1 - e^{-\sqrt{\frac{u}{D}}|z_0|} \right), \quad (10)$$

Taking the limit $u \rightarrow 0$ in Eq. (9) yields the mean first-passage time. It is possible to show that when the resetting occurs such that $z_i = z_0$ for all i , then the summation in Eq. (9) is a geometrical summation and the mean first-passage time obtained coincides with the result obtained in Ref. [1] for the problem of a static prey. In our case, z_i is a random variable and the problem becomes analytically intractable, since averages must be performed over the z_i 's, of unknown distributions. Nevertheless, we can approximate the sum in Eq. (9) by replacing z_i by its typical value $\sqrt{2D_y i}/Q$ (which corresponds to $\lambda \rightarrow \infty$, since the predator relocates to the initial position of the prey) and by truncating the summation to $n = 1$ and $n = 2$ for $Q\mathcal{T}_0 < 1$ and $Q\mathcal{T}_0 > 1$, respectively. This choice is motivated by our simulations in Fig. 4, where we have plotted the mean number of resets before the first-encounter *vs* the reset rate obtained from the simulations and an analytical approximation documented in the supplemental material [30]. Figure 3 displays the resulting mean first encounter times with solid lines, which show excellent agreement with the numerical simulation during seven orders of magnitude in the resetting rate Q .

Now notice that for $Q\mathcal{T}_0 < 1$ the two regimes depend on the predator chasing strategy (λ) whereas for $Q\mathcal{T}_0 > 1$ this dependence is lost as shown in Fig. 3. In addition, $\langle t \rangle$ diverges as $(Q\mathcal{T}_0)^{-1/2}$ for $Q\mathcal{T}_0 \rightarrow 0$, recovering the case at $Q = 0$. Around $Q\mathcal{T}_0 \sim 1$, a crossover to the scaling $(Q\mathcal{T}_0)^{-1}$ is observed for $Q\mathcal{T}_0 \gtrsim 1$. These two scaling regimes are also recovered from the exact analytical expression $\langle t \rangle = (1 - e^{-\sqrt{Q\mathcal{T}_0}})/Q$ for the case $\lambda \rightarrow -\infty$ (dashed line in Fig. 3) and from Eq. (9) by setting $z_i = 0$ for all i and taking the limit $u \rightarrow 0$.

Finally, as mentioned, from numerical simulations the average number of resets before the predator-prey encounter, increases from zero with Q and saturates to about 2.2 (for $\lambda \rightarrow -\infty$) and 1 (for $\lambda \rightarrow \infty$). We further derived an analytical approximation for the mean number of resets before the predator-prey's encounter

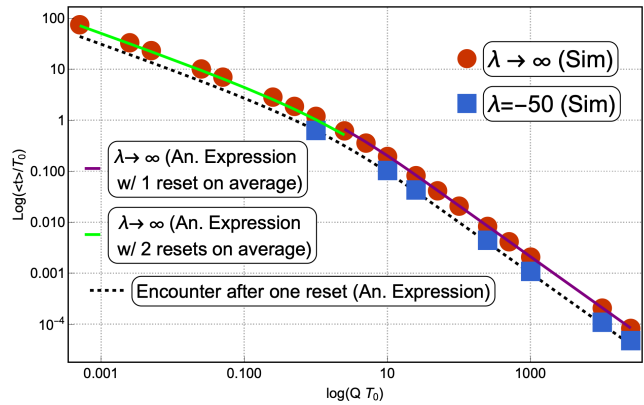


FIG. 3. Mean first-encounter time *vs* $Q\mathcal{T}_0$ for different values of λ (see legends). The dashed line corresponds to the short-term memory predator resetting strategy $\lambda \rightarrow -\infty$. The blue squares correspond to data obtained from numerical simulations with λ fixed at -50 and with time-step size ranging from 10^{-3} to 10^{-6} , depending on the value of Q . The red circles correspond to numerical simulations for which $\lambda \rightarrow \infty$. The continuous lines correspond to our approximate analytical result (see main text for discussion). Each data point corresponds to 10^7 simulations.

(see supplemental material in Ref. [30] for the analytical derivation). The solid lines in Fig. 4 corresponds to our analytical expression while the data points corresponds to simulations.

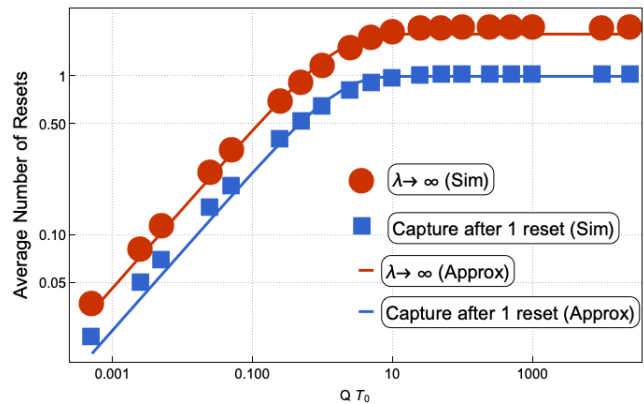


FIG. 4. Mean number of resets before the first encounter between the prey and predator *vs* Q for different values of λ (see legends). The data points were obtained from the simulations while the continuous lines correspond to our analytical results well documented in the SM in Ref. [30]. There is a threshold for the reset rate Q for which above that the mean number of resets before the first encounter saturate. Each point corresponds to 10^7 simulations.

In conclusion, we analyzed the distribution of a Brownian particle that resets to positions previously visited by another Brownian particle. This process depends on a memory function that accounts for the available infor-

mation of the previously visited locations of the prey. We have also studied the first encounter times in this problem. We showed that both particles meet in a finite time, independently of the chasing behavior, and decreases as the resetting rate increases. Additionally, the long-time diffusion behavior of the predator is slaved to the diffusion of the prey. When only information about the recent locations of the prey is available to the predator, the latter tends to mimic the diffusion process of the prey, and ends up diffusing with the prey's diffusion coefficient. If only information of the initial positions visited by the prey is available to the predator, the latter becomes trapped around the initial position of the prey. In contrast, if the the whole information is equally available the predator ends up diffusing with half the diffusivity of the prey.

F.J.S kindly acknowledges support from grant UNAM-DGAPA-PAPIIT-IN114717. JQTM acknowledges a doctoral fellowship from Consejo Nacional de Ciencia y Tecnología (México). JQTM gratefully thanks Gerardo G. Naumis, Reinaldo Garcia-Garcia, Mehran Kardar and James Glazier for discussions.

* j.toledo.mx@gmail.com

† boyer@fisica.unam.mx

‡ FJS; fjsevilla@fisica.unam.mx

- [1] M. R. Evans and S. N. Majumdar, Physical review letters **106**, 160601 (2011).
- [2] M. R. Evans and S. N. Majumdar, Journal of Physics A: Mathematical and Theoretical **44**, 435001 (2011).
- [3] M. R. Evans, S. N. Majumdar, and K. Mallick, *Journal of Physics A: Mathematical and Theoretical* **46**, 185001 (2013).
- [4] A. Pal and S. Reuveni, Physical review letters **118**, 030603 (2017).
- [5] A. Pal, A. Kundu, and M. R. Evans, Journal of Physics A: Mathematical and Theoretical **49**, 225001 (2016).
- [6] S. Reuveni, *Phys. Rev. Lett.* **116**, 170601 (2016).
- [7] M. R. Evans, S. N. Majumdar, and G. Schehr, arXiv preprint arXiv:1910.07993 (2019).
- [8] P. Krapivsky and S. Redner, J. Phys. A: Math. Gen. **29**, 5347 (1996).
- [9] S. Redner and P. Krapivsky, Am. J. Phys. **67**, 1277 (1999).
- [10] G. Oshanin, O. Vasilyev, P. Krapivsky, and J. Klafter, Proceedings of the National Academy of Sciences **106**, 13696 (2009).
- [11] A. Gabel, S. N. Majumdar, N. K. Panduranga, and S. Redner, JSTAT **2012**, P05011 (2012).
- [12] S. Redner and O. Bénichou, JSTAT **2014**, P11019 (2014).
- [13] M. Schwarzl, A. Godec, G. Oshanin, and R. Metzler, *Journal of Physics A: Mathematical and Theoretical* **49**, 225601 (2016).
- [14] A. Das and G. P. Samanta, *Journal of Physics A: Mathematical and Theoretical* **51**, 465601 (2018).
- [15] G. Mercado-Vásquez and D. Boyer, Journal of Physics A: Mathematical and Theoretical **51**, 405601 (2018).
- [16] S. D. Boie, E. G. Connor, M. McHugh, K. I. Nagel, G. B. Ermentrout, J. P. Crimaldi, and J. D. Victor, PLoS computational biology **14**, e1006275 (2018).
- [17] K. L. Baker, M. Dickinson, T. M. Findley, D. H. Gire, M. Louis, M. P. Suver, J. V. Verhagen, K. I. Nagel, and M. C. Smear, Journal of Neuroscience **38**, 9383 (2018).
- [18] M. Dangkulwanich, T. Ishibashi, S. Liu, M. L. Kireeva, L. Lubkowska, M. Kashlev, and C. J. Bustamante, *Elife* **2**, e00971 (2013).
- [19] É. Roldán, A. Lisica, D. Sánchez-Taltavull, and S. W. Grill, Physical Review E **93**, 062411 (2016).
- [20] Y. Zhang and O. K. Dudko, Annual review of biophysics **45**, 117 (2016).
- [21] D. Campos, F. Bartumeus, and V. m. c. Méndez, *Phys. Rev. E* **96**, 032111 (2017).
- [22] G. M. Viswanathan, M. G. E. da Luz, E. P. Raposo, and H. E. Stanley, *The Physics of Foraging: An Introduction to Random Searches and Biological Encounters* (Cambridge University Press, 2011).
- [23] V. Méndez, D. Campos, and F. Bartumeus, *Stochastic foundations in movement ecology: Anomalous Diffusion, Front Propagation and Random Searches*, Springer Series in Synergetics (Springer-Verlag Berlin Heidelberg, 2014).
- [24] T. Chou and M. R. D'Orsogna, in *First-Passage Phenomena and Their Applications* (World Scientific, 2014) pp. 306–345.
- [25] D. Krapf and R. Metzler, PHYSICS TODAY **72**, 48 (2019).
- [26] G. M. Schütz and S. Trimper, *Phys. Rev. E* **70**, 045101 (2004).
- [27] J. C. Cressoni, M. A. A. da Silva, and G. M. Viswanathan, *Phys. Rev. Lett.* **98**, 070603 (2007).
- [28] D. Boyer and C. Solis-Salas, Physical review letters **112**, 240601 (2014).
- [29] D. Boyer, M. R. Evans, and S. N. Majumdar, *Journal of Statistical Mechanics: Theory and Experiment* **2017**, 023208 (2017).
- [30] See Supplemental Material at [URL will be inserted by publisher] for a detailed derivation.
- [31] V. Sposini, A. V. Chechkin, F. Seno, G. Pagnini, and R. Metzler, *New Journal of Physics* **20**, 043044 (2018).
- [32] L. E. Elsgolts and G. Yankovsky, *Differential equations and the calculus of variations* (Mir Moscow, 1977).
- [33] S. Redner, *A guide to first-passage processes* (Cambridge University Press, 2001).

Derivation of Eqs. (5) and (6)

We explicitly found the solution of the Fokker-Planck equation (4) in the manuscript, namely

$$\begin{aligned} \frac{\partial}{\partial t} \Pi(x, t|x_0) &= D_x \frac{\partial^2}{\partial x^2} \Pi(x, t|x_0) - Q \Pi(x, t|x_0) \\ &+ Q \int_0^t ds \phi(s; t) P(x, s). \end{aligned} \quad (11)$$

After Fourier transforming this last equation we get

$$\begin{aligned} \frac{\partial}{\partial t} \hat{\Pi}(k, t|x_0) &= -D_x k^2 \frac{\partial^2}{\partial x^2} \hat{\Pi}(k, t|x_0) - Q \hat{\Pi}(k, t|x_0) \\ &+ Q \int_0^t ds \phi(s; t) \hat{P}(k, s), \end{aligned} \quad (12)$$

whose solution is given straightforwardly by

$$\begin{aligned} \Pi(x, t|x_0) &= e^{-Qt} \hat{G}_{D_x}(k, t) \hat{\Pi}(k, 0) \\ &+ Q \int_0^t ds e^{-Q(t-s)} \hat{G}_{D_x}(k, t-s) \\ &\times \int_0^s ds' \phi(s'; s) \hat{G}_{D_y}(k, s') e^{-iky_0}. \end{aligned} \quad (13)$$

where $\hat{G}_D(k, t) = \exp\{-D_x k^2 t\}$ is the Fourier transform of the Gaussian propagator

$$G_D(u, t|u_0) = \frac{1}{\sqrt{4\pi Dt}} \exp\left\{-\frac{(u-u_0)^2}{4Dt}\right\} \quad (14)$$

with diffusion coefficient D . By noticing that

$$\begin{aligned} \hat{G}_{D_x}(k, t) \hat{G}_{D_y}(k, s') e^{-iky_0} &= \\ \hat{G}_{D_y}\left(k, \frac{D_x}{D_y}(t-s) + s'\right) e^{-iky_0} \end{aligned} \quad (15)$$

we get the Eq. (5) of the manuscript, namely

$$\begin{aligned} \Pi(x, t|x_0) &= e^{-Qt} G_{D_x}(x, t|x_0) + Q \int_0^t ds e^{-Q(t-s)} \\ &\times \int_0^s ds' \phi(s'; s) G_{D_y}\left(x, \frac{D_x}{D_y}(t-s) + s' \middle| y_0\right), \end{aligned} \quad (16)$$

The analysis in the regime of long times, is easier from Eq. (13). In this regime, the first term in the right-hand side of can be neglected, while the second one can be evaluated by use of the *Markovian approximation*, i.e., by taking out the factor that depends on s' evaluated at $s = t$ multiplied by the integral over t from 0 to ∞ of $Q e^{-Qt} \hat{G}_{D_x}(k, t)$, i.e.,

$$\hat{\Pi}_\infty(k, t) \sim \frac{Q}{D_x k^2 + Q} \int_0^t ds \phi(s; t) \hat{G}_{D_y}(k, s) e^{-iky_0}. \quad (17)$$

Inversion of the Fourier transform leads to the equation (6) of the manuscript, where the Laplace distribution $L_{D_x/Q}(x) = \exp\{-|x|/l\}/2l$ appears as the Fourier inverse of $Q/[D_x k^2 + Q]$.

Explicit solutions for particular resetting strategies

Case $\lambda = 0$

We start by formally expressing the problem mathematically, i.e.,

$$\frac{\partial}{\partial t} P_0(y, t) = D_y \frac{\partial^2}{\partial y^2} P_0(y, t), \quad (18a)$$

$$\begin{aligned} \frac{\partial}{\partial t} P(x, t) &= D_x \frac{\partial^2}{\partial x^2} P(x, t) - Q P(x, t) \\ &+ Q \int_0^t dt' \phi(t, t') P_0(x, t'), \end{aligned} \quad (18b)$$

with initial conditions $P_0(y, 0) = \delta(y - y_0)$, $P(x, 0) = \delta(x - x_0)$ and kernel function $\phi(t, t') = 1/t$. The solution of Eq. (18a) is straightforward, namely,

$$P_0(y, t) = \frac{1}{\sqrt{4D_y \pi t}} \exp\left(-\frac{(y-y_0)^2}{4D_y t}\right). \quad (19)$$

Applying Fourier transform yields

$$P_0(q, t) = \exp(-q^2 D_y t - i q y_0) \quad (20)$$

Now, the general solution to Eq. (18b) may be expressed as,

$$P(k, t) = A(t) \exp(-(Q + k^2 D_x)t). \quad (21)$$

Then, when substituting the previous Eq. in the non-homogeneous Fokker-Planck Eq. and solving for $A(t)$ yields,

$$\begin{aligned} A(t) &= A(0) \\ &+ \int_0^t d\tau \exp((Q + k^2 D_x)\tau) \frac{Q e^{-iky_0}}{\tau k^2 D_y} \left(1 - e^{-k^2 D_y \tau}\right). \end{aligned} \quad (22)$$

Notice from the initial condition $A(0) = \exp(-ikx_0)$. Taking into account the integration constant and the previous Eq., $P(k, t)$ now reads

$$\begin{aligned} P(k, t) &= \exp(-(Q + k^2 D_x)t - ikx_0) \\ &+ \int_0^t d\tau \frac{Q e^{-iky_0}}{\tau k^2 D_y} \left(1 - e^{-k^2 D_y \tau}\right) \exp(-(Q + k^2 D_x)(t - \tau)) \end{aligned} \quad (23)$$

The first term on the r.h.s. of the last equality is simply the Fourier transform of the solution to the homogeneous Fokker-Planck Eq. multiplied by a decaying exponential which makes patent the loss in probability in the diffusive regime. Hence, in real space this yield,

$$P_h(x, t) = \frac{e^{-Qt}}{\sqrt{4\pi D_x t}} \exp\left(-\frac{(x-x_0)^2}{4D_x t}\right). \quad (24)$$

The second term is a little bit more complicated to transform into real space. Hence, we provide a detailed way in doing so. Let us first denote this term as $G(k, t)$. Hence,

$$G(k, t) = \int_0^t d\tau \frac{Q e^{Q(\tau-t)} e^{-iky_0}}{\tau k^2 D_y} \times \left(e^{-k^2 D_x(t-\tau)} - e^{-k^2(\tau(D_y - D_x) + D_x t)} \right). \quad (25)$$

To obtain the inverse Fourier transform of $G(k, t)$, we introduce an auxiliary problem. Let us compute the inverse Fourier transform of $\exp(-k^2 z)/k^2$. Hence, we define a function $F(x)$ such that,

$$F(x) = \frac{1}{2\pi} \int_{-\infty}^{\infty} dk \frac{e^{-k^2 z}}{k^2} e^{ikx}. \quad (26)$$

However, notice that

$$\frac{d^2 F(x)}{dx^2} = -\frac{1}{2\pi} \int_{-\infty}^{\infty} dk e^{-k^2 z} e^{ikx} \quad (27)$$

The r.h.s in the previous Eq. yields a Gaussian distribution centered at $x = 0$ and with root-mean-squared equal to $2z$. Therefore, integrating the above over x and fixing the integration constants to the function evaluated in zero yields:

$$\mathcal{F}^{-1} \left[\frac{e^{-k^2 z}}{k^2} \right] (x) \equiv F(x) = -\sqrt{\frac{z}{\pi}} e^{-\frac{x^2}{4z}} - \frac{1}{2} |x| \mathbf{Erf} \left(\frac{|x|}{2\sqrt{z}} \right). \quad (28)$$

We may now go back to our main concern, which is the function $G(k, t)$, and use the previous result by assuming $x \rightarrow x - y_0$. Hence, Eq. (25) becomes,

$$G(x, t) = \int_0^t d\tau \frac{Q e^{Q(\tau-t)}}{\tau D_y} \left(-\sqrt{\frac{D_x(t-\tau)}{\pi}} e^{-\frac{(x-y_0)^2}{4D_x(t-\tau)}} - \frac{1}{2} |x - y_0| \mathbf{Erf} \left(\frac{|x - y_0|}{2\sqrt{D_x(t-\tau)}} \right) + \sqrt{\frac{\tau(D_y - D_x) + D_x t}{\pi}} e^{-\frac{(x-y_0)^2}{4(\tau(D_y - D_x) + D_x t)}} + \frac{1}{2} |x - y_0| \mathbf{Erf} \left(\frac{|x - y_0|}{2\sqrt{\tau(D_y - D_x) + D_x t}} \right) \right). \quad (29)$$

By performing further algebra, one is able reduce the previous result to,

$$G(x, t) = \int_0^t d\tau \frac{Q e^{Q(\tau-t)}}{\tau D_y} \left(\sqrt{\frac{\tau(D_y - D_x) + D_x t}{\pi}} e^{-\frac{(x-y_0)^2}{4(\tau(D_y - D_x) + D_x t)}} - \sqrt{\frac{D_x(t-\tau)}{\pi}} e^{-\frac{(x-y_0)^2}{4D_x(t-\tau)}} - \frac{1}{2} |x - y_0| \mathbf{Erf} \left(\frac{|x - y_0|}{2\sqrt{\tau(D_y - D_x) + D_x t}}, \frac{|x - y_0|}{2\sqrt{D_x(t-\tau)}} \right) \right), \quad (30)$$

and

$$P(x, t) = \frac{e^{-Qt}}{\sqrt{4\pi D_x t}} \exp \left(-\frac{(x - x_0)^2}{4D_x t} \right) + G(x, t). \quad (31)$$

This result was compared with simulations and it is shown in Fig. 5.

Case $\lambda < 0$

where

Let us first denote $\rho = -\lambda$. Now, we are interested in the explicit solution to Eqs. (18) with the same initial conditions as in the previous case but with a kernel function,

$$\phi(t, t') = \frac{e^{-\rho(t-t')}}{\Lambda(t)}, \quad (32)$$

$$\Lambda(t) = \frac{1 - e^{-\rho t}}{\rho}, \quad (33)$$

we are interested in the real-space representation of

$$P(k, t) = e^{-(Q+k^2 D_x)t - ikx_0} + \frac{Q\rho e^{-iky_0}}{k^2 D_y - \rho} \int_0^t d\tau \frac{1 - e^{-(k^2 D_y - \rho)\tau}}{e^{\rho\tau} - 1} e^{(Q+k^2 D_x)\tau} e^{-(Q+k^2 D_x)t}.$$

We do this in a similar manner to that in the previous case. For this purpose, let us first derive a formula which will be very useful. Let us suppose we are interested in the following integral,

$$F(x; a, b, A, \mathcal{D}) = \int_{-\infty}^{\infty} \frac{dk}{2\pi} \frac{e^{-k^2 a} - e^{-k^2 b + A}}{k^2 - \mathcal{D}} e^{ikx}. \quad (35)$$

Let us define,

$$g(x; a, b, A) = - \int_{-\infty}^{\infty} \frac{dk}{2\pi} \left(e^{-k^2 a} - e^{-k^2 b + A} \right) e^{ikx}. \quad (36)$$

Therefore, the function $F(x)$ satisfies the following differential equation,

$$F''(x) + DF(x) = g(x). \quad (37)$$

Now, to solve the previous Eq., one might be tempted in using Fourier Transform method. However, that would take us back to our starting point. Hence, we use the pa-

rameter variation method [32]. Thus, the solution yields

$$F(x; a, b, A, \mathcal{D}) = c_1(x) \cos(\sqrt{\mathcal{D}}x) + c_2(x) \sin(\sqrt{\mathcal{D}}x). \quad (38)$$

where,

$$(34) \quad \begin{cases} c_2(x; a, b, A, \mathcal{D}) = \int_0^x dx' \frac{g(x') \cos(\sqrt{\mathcal{D}}x')}{\sqrt{\mathcal{D}}}, \\ c_1(x; a, b, A, \mathcal{D}) = - \int_{-\infty}^x dx' \frac{g(x') \sin(\sqrt{\mathcal{D}}x')}{\sqrt{\mathcal{D}}}. \end{cases} \quad (39)$$

Notice that we have chosen different integration limits. The reason will become clear later on. Therefore, we have

$$F(x; a, b, A, \mathcal{D}) = - \int_{-\infty}^x dx' \frac{g(x') \sin(\sqrt{\mathcal{D}}x')}{\sqrt{\mathcal{D}}} \cos(\sqrt{\mathcal{D}}x) + \int_0^x dx' \frac{g(x') \cos(\sqrt{\mathcal{D}}x')}{\sqrt{\mathcal{D}}} \sin(\sqrt{\mathcal{D}}x). \quad (40)$$

Notice that when \mathcal{D} and A tend to 0, the previous Eq. becomes

$$F(x; a, b, A, \mathcal{D}) = \frac{\sqrt{b}}{\sqrt{\pi}} e^{-\frac{x^2}{4b}} - \frac{\sqrt{a}}{\sqrt{\pi}} e^{-\frac{x^2}{4a}} - \frac{x}{2} \left(\mathbf{Erf} \left(\frac{x}{\sqrt{4b}}, \frac{x}{\sqrt{4a}} \right) \right). \quad (41)$$

In agreement with the case in the previous section. Let us return to to Eq. (34) and rewrite it as

$$P(k, t) = e^{-(Q+k^2 D_x)t - ikx_0} + \int_0^t d\tau \frac{Q\rho e^{-Q(t-\tau)}}{(e^{\rho\tau} - 1) D_y} e^{-iky_0} F(k; D_x(t - \tau), D_y\tau + D_x(t - \tau), \rho\tau, \rho/D_y). \quad (42)$$

Using the previous results leads to

$$P(x, t) = \frac{e^{-Qt} e^{-\frac{(x-x_0)^2}{4D_x t}}}{\sqrt{4\pi D_x t}} + \int_0^t d\tau \frac{Q\rho e^{-Q(t-\tau)}}{(e^{\rho\tau} - 1) D_y} F(x - y_0; D_x(t - \tau), D_y\tau + D_x(t - \tau), \rho\tau, \rho/D_y) \quad (43)$$

Let us now check the normalization condition in the previous Eq. by integrating over the real axis:

$$1 = \int_{-\infty}^{\infty} dx P(x, t) = e^{-Qt} + \int_0^t d\tau \frac{Q\rho e^{-Q(t-\tau)}}{(e^{\rho\tau} - 1) D_y} \int_{-\infty}^{\infty} dx F(x - y_0; D_x(t - \tau), D_y\tau + D_x(t - \tau), \rho\tau, \rho/D_y) \quad (44)$$

Now, the dependence on x in the second term is solely because of $F(x)$. Therefore, let us integrate $F(x)$. Let us denote the terms in $F(x)$ as

$$\begin{cases} G_s(x) = \int_{-\infty}^x dx' \frac{g(x') \sin(\sqrt{\mathcal{D}}x')}{\sqrt{\mathcal{D}}}, \\ G_c(x) = \int_0^x dx' \frac{g(x') \cos(\sqrt{\mathcal{D}}x')}{\sqrt{\mathcal{D}}}, \end{cases} \quad (45)$$

Thus,

$$\int_{-\infty}^{\infty} dx F(x) = - \int_{-\infty}^{\infty} G_s(x) \cos(\sqrt{\mathcal{D}}x) + \int_{-\infty}^{\infty} G_c(x) \sin(\sqrt{\mathcal{D}}x). \quad (46)$$

Integrating by parts and taking into account that $dG_s(x)/dx$ is an odd function, yields

$$\int_{-\infty}^{\infty} dx F(x) = \frac{1}{\mathcal{D}} \int_{-\infty}^{\infty} g(x) + \frac{G_c(x) \cos(\sqrt{\mathcal{D}}x)}{\sqrt{\mathcal{D}}} \Big|_{-\infty}^{\infty}. \quad (47)$$

It is not difficult to see that the last term is zero, given the way we have chosen the integration limits of $G_c(x)$.

Hence,

$$\int_{-\infty}^{\infty} dx F(x) = \frac{1}{\mathcal{D}} \int_{-\infty}^{\infty} g(x) = \frac{1}{\mathcal{D}} (e^A - 1). \quad (48)$$

Plugging this in Eq. (44) with $A = \rho\tau$ and $\mathcal{D} = \rho/D_y$, fulfills the equality. The integrals in the previous results may further be put in terms of Error and Dawson functions. Before carrying on, let us first write some useful identities, namely:

$$\begin{aligned} \int_0^x dx' \frac{e^{-\frac{x'^2}{4\alpha}}}{\sqrt{4\pi\alpha}} e^{\pm ikx'} &= \frac{e^{-k^2\alpha}}{2} \mathbf{Erf} \left(\mp i\sqrt{\alpha}k, \frac{x \mp i2\alpha k}{\sqrt{4\alpha}} \right), \\ \int_0^x dx' \frac{e^{-\frac{x'^2}{4\alpha}}}{\sqrt{4\pi\alpha}} \cos kx' &= \frac{1}{2} \frac{e^{-k^2\alpha}}{2} \left(\mathbf{Erf} \left(\frac{x - i2\alpha k}{\sqrt{4\alpha}} \right) + \mathbf{Erf} \left(\frac{x + i2\alpha k}{\sqrt{4\alpha}} \right) \right), \\ \int_0^x dx' \frac{e^{-\frac{x'^2}{4\alpha}}}{\sqrt{4\pi\alpha}} \sin kx' &= \frac{1}{2i} \frac{e^{-k^2\alpha}}{2} \left(\mathbf{Erf} \left(-i\sqrt{\alpha}k, \frac{x - i2\alpha k}{\sqrt{4\alpha}} \right) - \mathbf{Erf} \left(i\sqrt{\alpha}k, \frac{x + i2\alpha k}{\sqrt{4\alpha}} \right) \right), \\ \int_0^{\infty} dx' \frac{e^{-\frac{x'^2}{4\alpha}}}{\sqrt{4\pi\alpha}} \sin kx' &= \frac{\mathbf{D}_+(k\sqrt{\alpha})}{\sqrt{\pi}}. \end{aligned} \quad (49)$$

Here, $\mathbf{D}_+(x)$ is the Dawson function. Hence, each of the terms in the function $F(x; a, b, A, \mathcal{D})$ may be expressed in terms of the previous Eqs., i.e.,

$$\int_0^x dx' \frac{g(x') \cos(\sqrt{\mathcal{D}}x')}{\sqrt{\mathcal{D}}} = \frac{1}{4\sqrt{\mathcal{D}}} \left(e^{A-\mathcal{D}b} \left(\mathbf{Erf} \left(\frac{x - i2b\sqrt{\mathcal{D}}}{\sqrt{4b}} \right) + \mathbf{Erf} \left(\frac{x + i2b\sqrt{\mathcal{D}}}{\sqrt{4b}} \right) \right) - e^{-\mathcal{D}a} \left(\mathbf{Erf} \left(\frac{x - i2a\sqrt{\mathcal{D}}}{\sqrt{4a}} \right) + \mathbf{Erf} \left(\frac{x + i2a\sqrt{\mathcal{D}}}{\sqrt{4a}} \right) \right) \right) \quad (50)$$

$$\begin{aligned} \int_0^x dx' \frac{g(x') \sin(\sqrt{\mathcal{D}}x')}{\sqrt{\mathcal{D}}} &= \frac{i}{4\sqrt{\mathcal{D}}} \left(e^{A-\mathcal{D}b} \left(-\mathbf{Erf} \left(\frac{x - i2b\sqrt{\mathcal{D}}}{\sqrt{4b}} \right) + \mathbf{Erf} \left(\frac{x + i2b\sqrt{\mathcal{D}}}{\sqrt{4b}} \right) - 2\mathbf{Erf}(i\sqrt{\mathcal{D}}b) \right) - e^{-\mathcal{D}a} \left(-\mathbf{Erf} \left(\frac{x - i2a\sqrt{\mathcal{D}}}{\sqrt{4a}} \right) + \mathbf{Erf} \left(\frac{x + i2a\sqrt{\mathcal{D}}}{\sqrt{4a}} \right) - 2\mathbf{Erf}(i\sqrt{\mathcal{D}}a) \right) \right) \end{aligned} \quad (51)$$

$$\int_{-\infty}^0 dx' \frac{g(x') \sin(\sqrt{\mathcal{D}}x')}{\sqrt{\mathcal{D}}} = -\frac{1}{\sqrt{\mathcal{D}}\pi} \left(e^A \mathcal{D}_+(\sqrt{\mathcal{D}}b) - \mathcal{D}_+(\sqrt{\mathcal{D}}a) \right). \quad (52)$$

Therefore, after some algebra, we obtain

$$F(x; a, b, A, \mathcal{D}) = \frac{e^{A-\mathcal{D}b}}{\sqrt{4\mathcal{D}}} \mathbf{Im} \left[\mathbf{Erf} \left(\frac{x + i2b\sqrt{\mathcal{D}}}{\sqrt{4b}} \right) e^{i\sqrt{\mathcal{D}}x} \right] - \frac{e^{\mathcal{D}a}}{\sqrt{4\mathcal{D}}} \mathbf{Im} \left[\mathbf{Erf} \left(\frac{x + i2a\sqrt{\mathcal{D}}}{\sqrt{4a}} \right) e^{i\sqrt{\mathcal{D}}x} \right]. \quad (53)$$

Thus, by putting the parameters $a = D_x(t - \tau)$, $b = D_y\tau + D_x(t - \tau)$, $A = \rho\tau$ and $\mathcal{D} = \rho/D_y$, we obtain:

$$F(x - y_0; D_x(t - \tau), D_y\tau + D_x(t - \tau), \rho\tau, \rho/D_y) = \frac{e^{\rho\tau - \rho(D_y\tau + D_x(t - \tau))/D_y}}{\sqrt{4\rho/D_y}}$$

$$\text{Im} \left[\text{Erf} \left(\frac{x - y_0 + i2(D_y\tau + D_x(t - \tau))\sqrt{\rho/D_y}}{\sqrt{4(D_y\tau + D_x(t - \tau))}} \right) e^{i\sqrt{\rho}(x - y_0)/\sqrt{D_y}} \right]$$

$$- \frac{e^{-\rho D_x(t - \tau)/D_y}}{\sqrt{4\rho/D_y}} \text{Im} \left[\text{Erf} \left(\frac{x - y_0 + i2D_x(t - \tau)\sqrt{\rho/D_y}}{\sqrt{4D_x(t - \tau)}} \right) e^{i\sqrt{\rho}(x - y_0)/\sqrt{D_y}} \right],$$

and

$$P(x, t) = \frac{e^{-Qt} e^{-\frac{(x - x_0)^2}{4D_x t}}}{\sqrt{4\pi D_x t}} + \int_0^t d\tau \frac{Q\rho e^{-Q(t - \tau)}}{(e^{\rho\tau} - 1)D_y} F(x - y_0; D_x(t - \tau), D_y\tau + D_x(t - \tau), \rho\tau, \rho/D_y). \quad (54)$$

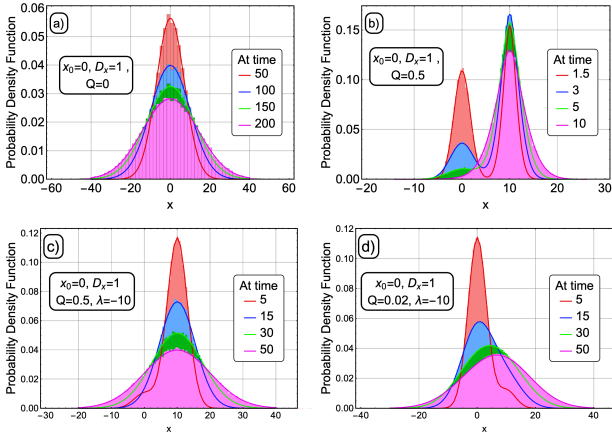


FIG. 5. (Color online) Dimensionless probability density function $l_y\Pi(x, t|x_0)$ as function of the dimensionless predator position x/l_y , with $l_y = \sqrt{D_y/Q}$. The bars correspond to the histograms obtained from numerical simulations, while solid lines mark the analytical result (54) and (31) (see legends). The simulations were performed fixing the parameters $D_x = D_y$, $x_0 = 0$, $y_0 = 10$, $dt = 0.001$ and on a sample size 10^4 . Each panel corresponds to a fixed reset rate Q and the different curves within a panel correspond to a different time snapshot of the process, as shown in the legends. Notice as Q increases, the peak shifts towards y_0 and becomes sharper.

This result was compared with simulations and it is shown in Fig. 5.

Mean value and mean squared displacement

Let us derive the mean value and the mean squared displacement (MSD). There are several ways on doing this, yet a simple way consists in multiplying the Fokker-Planck Eq. by x^n , integrating it over the Real line and then solving the resulting differential equation. In the case of the mean value, we must solve the following dif-

ferential Eq.

$$\frac{d\langle x(t) \rangle}{dt} = -Q\langle x(t) \rangle + Q \int_0^t dt' \phi(t, t') y_0 = -Q\langle x(t) \rangle + Q y_0. \quad (55)$$

The solution to the previous Eq. is quite simple and independent of the memory kernel, i.e.,

$$\langle x(t) \rangle = x_0 e^{-Qt} + y_0 (1 - e^{-Qt}). \quad (56)$$

For the MSD, denoting $\eta(t) = \langle x^2(t) \rangle$ to simplify notation, following the same procedure we obtain the following differential Eq.

$$\frac{d\langle x^2(t) \rangle}{dt} = -Q\langle x^2(t) \rangle + 2D_x + Q \int_0^t dt' \phi(t, t') (y_0^2 + 2D_y t'). \quad (57)$$

The solution is straightforward, namely,

$$\langle x^2(t) \rangle_{\lambda < 0} = x_0^2 e^{-Qt} + y_0^2 (1 - e^{-Qt}) + \frac{2D_x}{Q} (1 - e^{-Qt}) + \frac{2D_y}{\lambda} (1 - e^{-Qt}) + 2QD_y \mathcal{X}(t, Q, \lambda, 0) \quad (58)$$

$$\langle x^2(t) \rangle_{\lambda = 0} = x_0^2 e^{-Qt} + y_0^2 (1 - e^{-Qt}) + D_y t + \frac{2D_x - D_y}{Q} (1 - e^{-Qt}) \quad (59)$$

$$\langle x^2(t) \rangle_{\lambda > 0} = x_0^2 e^{-Qt} + y_0^2 (1 - e^{-Qt}) + \frac{2D_x}{Q} (1 - e^{-Qt}) + \frac{2D_y}{\lambda} (1 - e^{-Qt}) - 2QD_y \mathcal{X}(t, Q, \lambda, 1) \quad (60)$$

where we define the function $\mathcal{X}(t, Q, \lambda, n_0)$ as,

$$\mathcal{X}(t, Q, \lambda, n_0) = \sum_{n=n_0}^{\infty} \frac{e^{-Qt} - e^{-|\lambda|nt} (1 - t(Q - |\lambda|n))}{(Q - |\lambda|n)^2} \times (1 - \mathbf{1}_{Q, n|\lambda|}) + \frac{t^2 e^{-Qt}}{2} \mathbf{1}_{Q, n|\lambda|}. \quad (61)$$

These expressions were compared with simulations and are shown in Fig. 2 of the main text.

Mean First Passage Time

In this section we show the method used to compute the first passage time. Let us denote as $z = x - y$ the relative distance between the prey and the predator. Notice that the encounter between the prey and the predator corresponds to $z = 0$. First, let us consider the situation in which $Q = 0$. It is widely known that in this case the survival probability is [33],

$$\mathcal{S}(z_0, t) = \text{Erf} \left(\frac{z_0}{\sqrt{4Dt}} \right). \quad (62)$$

Here $z_0 = x_0 - y_0$ is the initial position and $D = D_x + D_y$. Now, let us assume $Q \neq 0$ and that only one reset occurs to $z = z_1$. Then, the survival probability of the whole process is, in fact, the convolution of the subprocess before the reset multiplied by the probability the reset does not occur and the subprocess after the reset multiplied, again, by the probability the reset does not occur. Although we are considering only one reset, we include the probability the reset does not occur in both terms of the convolution because in the end we will consider the limit for infinite number of resets. Therefore, the previous ideas yield the following:

$$\begin{aligned} \mathcal{S}^{(1)}(z_0, z_1, t) &= Q \int_0^t dt_1 e^{-Qt_1} \mathcal{S}(z_1, t_1) \\ &\times \int_0^t dt_0 e^{-Qt_0} \mathcal{S}(z_0, t_0) \delta(t - t_1 - t_0) \end{aligned} \quad (63)$$

Generalizing to n resets is straightforward. Hence, for n resets we may write,

$$\begin{aligned} \mathcal{S}^{(n)}(z_0, \{z_i\}, t) &= \prod_{i=1}^n \int_0^t dt_i e^{-Qt_i} Q \mathcal{S}(z_i, t_i) \\ &\times \int_0^t dt_0 e^{-Qt_0} \mathcal{S}(z_0, t_0) \delta \left(t - \sum_{i=0}^n t_i \right). \end{aligned} \quad (64)$$

Now, applying Laplace transform, which we denote with a $\tilde{\bullet}$, on the previous Eq. (64) yields

$$\tilde{\mathcal{S}}^{(n)}(z_0, \{z_i\}, u) = \prod_{i=1}^n [Q \tilde{\mathcal{S}}(z_i, u + Q)] \tilde{\mathcal{S}}(z_0, Q + u). \quad (65)$$

The survival probability given any number of resets, $\mathcal{S}_Q^{(n)}$, yields

$$\begin{aligned} \tilde{\mathcal{S}}_Q(z_0, \{z_i\}, u) &= \tilde{\mathcal{S}}(z_0, Q + u) + \sum_{n=1}^{\infty} \tilde{\mathcal{S}}^{(n)}(z_0, u) \\ &= \tilde{\mathcal{S}}(z_0, Q + u) \left(1 + \sum_{n=1}^{\infty} \prod_{i=1}^n [Q \tilde{\mathcal{S}}(z_i, u + Q)] \right). \end{aligned} \quad (66)$$

From the Laplace transform of the survival probability one may obtain the mean first passage time by taking

the limit $u \rightarrow 0$. Moreover, the Laplace transform of the survival probability given that there is no reset (see Eq. (62)) yields,

$$\tilde{\mathcal{S}}_Q(z_0, u) = \frac{1}{u} \left(1 - \exp \left(-\sqrt{\frac{u}{D}} |z_0| \right) \right). \quad (67)$$

Thus, Eq. (66) becomes,

$$\begin{aligned} \tilde{\mathcal{S}}_Q(z_0, \{z_i\}, u) &= \frac{1}{Q + u} \left(1 - e^{-\sqrt{\frac{u+Q}{D}} |z_0|} \right) \\ &\left(1 + \sum_{n=1}^{\infty} \prod_{i=1}^n \left[\frac{Q}{Q + u} \left(1 - e^{-\sqrt{\frac{u+Q}{D}} |z_i|} \right) \right] \right). \end{aligned} \quad (68)$$

Let us now consider some well-known scenarios to support the usefulness of Eq. (68). First, notice that Eq. (68) diverges in the limit when $Q \rightarrow 0$ and $u \rightarrow 0$, in agreement with the mean first passage time when there are no resets. Now, recall that z_i is the relative distance once the i^{th} reset takes place. Then, for the case where $\lambda \rightarrow -\infty$, i.e., the predator resets to the present position of the prey, we have $z_i = 0$ for all i . Thus, Eq. (68) becomes,

$$\tilde{\mathcal{S}}_Q(z_0, \{0\}, u) = \frac{1}{Q + u} \left(1 - e^{-\sqrt{\frac{u+Q}{D}} |z_0|} \right). \quad (69)$$

The mean first passage time yields, by taking the limit $u \rightarrow 0$,

$$\langle t \rangle_{\lambda \rightarrow -\infty} = \frac{1}{Q} \left(1 - e^{-\sqrt{\frac{Q}{D}} |z_0|} \right). \quad (70)$$

which may also be obtained by a backward-Fokker-Planck procedure. Additionally, the previous Eq. has been plotted in Fig. 3 of the main text.

Another interesting case corresponds to when $z_i = z_0$ for all i which means that the relative distance is always the same after each reset, then Eq. (68) becomes

$$\begin{aligned} \tilde{\mathcal{S}}_Q(z_0, \{z_i\}, u) &= \frac{1}{Q + u} \left(1 - e^{-\sqrt{\frac{u+Q}{D}} |z_0|} \right) \\ &\left(1 + \sum_{n=1}^{\infty} \left[\frac{Q}{Q + u} \left(1 - e^{-\sqrt{\frac{u+Q}{D}} |z_i|} \right) \right]^n \right). \end{aligned} \quad (71)$$

The summation in the previous Eq. is a geometric summation and term inside is between 0 and 1, hence, the summation converges. It is possible to show that taking the limit $u \rightarrow 0$ yields the mean first passage time of a Brownian particle hitting the origin given that it resets to the same position with rate Q , namely,

$$\langle t \rangle_{\forall_i z_i = z_0} = \frac{1}{Q} \left(e^{\sqrt{\frac{Q}{D}} |z_0|} - 1 \right), \quad (72)$$

In perfect agreement with Ref. [1]. Now, the actual value of $\mathcal{S}(z_0, \{z_i\}, u)$ and, thus, the mean first passage

time will depend on the actual values of z_i which are random variables. Hence, the exact result would be rather cumbersome to obtain. We, however, circumvent this issue by truncating the summation up to the mean number of resets for the first encounter. In the following section we discuss this.

Mean number of resets

In this section we show the derivation to obtain the mean number of resets for the first encounter for $\lambda \rightarrow \pm\infty$. Let us first consider the case $\lambda \rightarrow -\infty$, i.e., the predator relocates to the present position of the prey when the reset occurs. Notice that the mean time between resets is simply $1/Q$ and, henceforth, we consider this approximation in our derivations. Therefore, in a coarse-grained approximation, we may think of the probability of first encounter before the first (and only) reset occurs, which we denote as $p(Q)$, given by,

$$p(Q) = \int_0^{1/Q} \frac{|z_0|}{\sqrt{4\pi Dt^3}} e^{-\frac{z^2}{4Dt}} = \mathbf{Erfc} \left(\frac{|z_0|}{2} \sqrt{\frac{Q}{D}} \right). \quad (73)$$

Conversely, the probability of first encounter after the first reset would be the probability the encounter did not happen before the first encounter, $1 - p(Q)$, multiplied by the probability the encounter occurred after the first reset, which is equal to 1 given that $\lambda \rightarrow -\infty$. It is trivial to show that the probability for the encounter happening before or after the first reset is equal to 1. Then, the mean number of reset for the first encounter, $\langle n(Q, \lambda \rightarrow -\infty) \rangle$, is given by,

$$\langle n(Q, \lambda \rightarrow -\infty) \rangle = 1 - p(Q). \quad (74)$$

In Fig. 4 of the main text we compare Eq. (74) with the mean number of resets before the first encounter obtained from our simulations.

Let us now turn our attention to the case where $\lambda \rightarrow \infty$, i.e., the predator always resets to the initial position of the prey. The pathway is the same as in the previous case. In order to simplify the derivation, it is helpful to consider a large but finite number of resets. Then, the first encounter probability after the first reset and before the second reset is given by,

$$P(n=1) = \mathbf{Erf} \left(\frac{|z_0|}{2} \sqrt{\frac{Q}{D}} \right) \mathbf{Erfc} \left(\frac{|z_1|}{2} \sqrt{\frac{Q}{D}} \right) \times A(n, z_2, \dots, z_N). \quad (75)$$

The first term in Eq. (75) corresponds to the non-encounter probability before the first reset whereas the second term corresponds to the encounter probability between the first and second reset. The last term corresponds to the probability of encounter after the second

reset and takes into account all possible combination. In the case where $z_i = z_0$ for all $i > 0$ it is trivial to show that the last term is $(p(Q) + (1 - p(Q)))^N = 1$. In the present case, the exact form of $A(n, \{z_i\})$ takes into account all the encounter probabilities after the second reset and is rather complex since it depends on the actual values of $\{z_i\}$. In any case, by normalization the value must be equal to 1. Then, the probability of first encounter after the m th reset and before the m th+1 is given by,

$$P(m) = \mathbf{Erf} \left(\frac{|z_0|}{2} \sqrt{\frac{Q}{D}} \right) \prod_{i=1}^{m-1} \left(\mathbf{Erf} \left(\frac{|z_i|}{2} \sqrt{\frac{Q}{D}} \right) \right) \times \mathbf{Erfc} \left(\frac{|z_m|}{2} \sqrt{\frac{Q}{D}} \right). \quad (76)$$

The mean number of resets for the first encounter, $\langle n(Q, \lambda \rightarrow \infty) \rangle$, is simply,

$$\langle n(Q, \lambda \rightarrow \infty) \rangle = \sum_{m=0}^{\infty} P(m)m. \quad (77)$$

We may further ask *How many resets are required for the first encounter to happen?* To this end, we compute the cumulative of Eq. (76). The fact of the matter is that the z_i are random variables, thus, in principle, one needs to average over these variables. To circumvent this issue, we consider z_i to be Gaussian random variables with mean squared displacement equal to $\sqrt{2D_y i/Q}$ and then we use the saddle point method. Therefore, we obtain,

$$P_{sp}(m) = \mathbf{Erf} \left(\frac{|z_0|}{2} \sqrt{\frac{Q}{D}} \right) \times \prod_{i=1}^{m-1} \left(\sqrt{\frac{Q}{2D_y \frac{d^2 B_i(z)}{dz^2} \Big|_{z=z^*}}} e^{-B_i(z^*)} \right) \times \left(1 - \sqrt{\frac{Q}{2D_y \frac{d^2 B_m(z)}{dz^2} \Big|_{z=z^*}}} e^{-B_m(z^*)} \right), \quad (78)$$

where

$$B_i(z) = \frac{z^2 Q}{4D_y i} - \log \left(\mathbf{Erf} \left(\frac{|z|}{2} \sqrt{\frac{Q}{D}} \right) \right). \quad (79)$$

We denote as $z = z^*$ the value for which the derivative of $B_i(z)$ with respect to z equates to zero. Using Eq. (78) we construct the cumulative of first encounter, i.e., $\sum P_{sp}(m)$ and we plot this in Fig. 6 to answer the aforementioned question. Notice that after two resets, the cumulative saturates regardless of the value of Q .

Using Eq. (77) together with Eqs. (75) and (76) we are able to give an approximation for the mean number of resets for the first encounter. Additionally, we made the approximation $z_i = \sqrt{2D_y i/Q}$ and we compared it with our simulations in Fig. 4 of the main text for a wide range of values of Q and the agreement is very good.

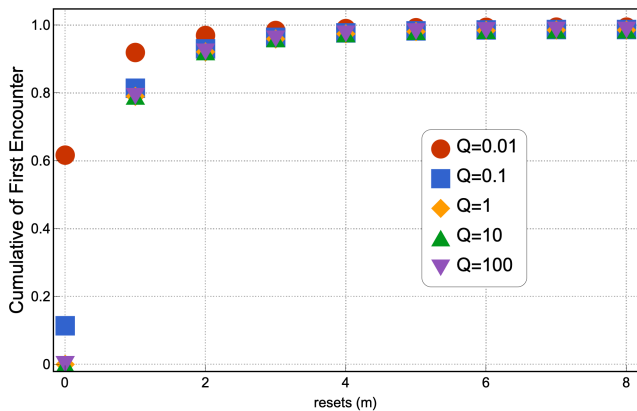


FIG. 6. Cumulative of the first encounter probability *vs* the number of resets, for different values of Q (see legend). Notice that for $Q \geq 0.1$ the curves collapse at $m = 2$, which is right before the cumulative saturates. On the other hand, for $Q = 0.01$, the cumulative saturates before. This implies that after 3 resets, the first encounter probability is essentially 1. This explains why the mean number of resets for the first encounter reaches a plateau as shown in Fig. 4 of the main text and, hence, supports the approximation of truncating the infinite sum in Eq. (11) of the main text. This result was obtained using the saddle point method (see text for further details).

Numerical simulations

In this section we describe the implementation our simulations. We first discretized the Langevin Eqs. shown in the main text. In the case where no capture was considered we ran the simulations for different Q values and negative values of λ . These results were then compared

with Eqs. (54) and (31) in Fig. 2 of the main text and shows excellent agreement. We then used this simulation for the statistics of the first encounter time. However, in order to correctly sample between resets, the time step of the simulation has to be much smaller than the characteristic reset time, $1/Q$, to properly sample between resets. This then leads to a rather dynamical time step and, additionally, as the time step decreases the computational time increases. Thus, going in this direction implies a trade-off between correct sampling and computational time. For these reasons, we instead performed a Kinetic Monte Carlo type simulation which reduces the computational time significantly and is fairly easy to implement for the cases $\lambda \rightarrow \pm\infty$.

First, we generate a first passage time random variable, t_0 , given the initial relative distance z_0 , between the predator and the prey, from a Lévy-Smirnov distribution as well as a reset time random variable τ_0 , given the fixed reset rate Q , from a Poisson distribution. Then, if $t_0 > \tau_0$, we keep repeating the previous step and denote the new first passage random variable as t_n obtained from a Lévy-Smirnov distribution, given a new relative distance right after the reset, z_n , and the new reset time random variable as τ_n , where n denotes the number of reset events that have occurred since the process started. If $t_n < \tau_n$, then the process stops and the first passage time random variable for that sample is $\sum_{i=0}^{n-1} \tau_i + t_n$. In general, the z_n 's are also random variables with unknown distributions. But, in the case where $\lambda \rightarrow -\infty$, $z_n = 0$ for all $n > 0$, conversely when $\lambda \rightarrow \infty$, then z_n is a Gaussian random variable with mean equal to zero and mean squared displacement equal to $2D_y \sum_{i=0}^{n-1} \tau_i$. The results were then compared with our analytical approximation in Fig. 3 in the main text.